




Quantitative assessment of sciatic nerve changes in Charcot–Marie–Tooth type 1A patients using magnetic resonance neurography

E. Fortanier^a, A. C. Ogier^{b,c} , E. Delmont^{a,d} , M.-N. Lefebvre^e, P. Viout^b, M. Guye^b, D. Bendahan^b  and S. Attarian^{a,f}

^aNeurology Department, APHM, Reference Center for Neuromuscular Diseases and ALS, La Timone University Hospital, Aix-Marseille University, Marseille; ^bCNRS, Center for Magnetic Resonance in Biology, UMR 7339, Aix-Marseille University, Marseille; ^cCNRS, LIS, Aix Marseille University, Toulon University, Marseille; ^dUMR 7286, Aix-Marseille University, Marseille; ^eAPHM, CIC-CPCE, La Timone University Hospital, Aix-Marseille University, Marseille; and ^fInserm, GMGF, Aix-Marseille University, Marseille, France

Keywords:

Charcot–Marie–Tooth type 1A, MRI, muscle, neurography, quantitative

Received 20 January 2020
Accepted 23 April 2020

European Journal of Neurology 2020, **0**: 1–8

doi:10.1111/ene.14303

Background and purpose: Nerve tissue alterations have rarely been quantified in Charcot–Marie–Tooth type 1A (CMT1A) patients. The aim of the present study was to quantitatively assess the magnetic resonance imaging (MRI) anomalies of the sciatic and tibial nerves in CMT1A disease using quantitative neurography MRI. It was also intended to seek for correlations with clinical variables.

Methods: Quantitative neurography MRI was used in order to assess differences in nerve volume, proton density and magnetization transfer ratio in the lower limbs of CMT1A patients and healthy controls. Disease severity was evaluated using the Charcot–Marie–Tooth Neuropathy Score version 2, Charcot–Marie–Tooth examination scores and Overall Neuropathy Limitations Scale scores. Electrophysiological measurements were performed in order to assess the compound motor action potential and the Motor Unit Number Index. Clinical impairment was evaluated using muscle strength measurements and Charcot–Marie–Tooth examination scores.

Results: A total of 32 CMT1A patients were enrolled and compared to 13 healthy subjects. The 3D nerve volume, magnetization transfer ratio and proton density were significantly different in CMT1A patients for the whole sciatic and tibial nerve volume. The sciatic nerve volume was significantly correlated with the whole set of clinical scores whereas no correlation was found between the tibial nerve volume and the clinical scores.

Conclusion: Nerve injury could be quantified *in vivo* using quantitative neurography MRI and the corresponding biomarkers were correlated with clinical disability in CMT1A patients. The sensitivity of the selected metrics will have to be assessed through repeated measurements over time during longitudinal studies to evaluate structural nerve changes under treatment.

Introduction

Charcot–Marie–Tooth (CMT) disease represents a heterogeneous group of inherited neuropathies [1]. CMT type 1A (CMT1A) is the most frequent

phenotype with an estimated prevalence of 1 in 5000 [2] and is characterized by a length-dependent sensory–motor deficit with distal muscle weakness and atrophy starting in childhood. This autosomal dominant demyelinating neuropathy is due to a DNA duplication in chromosome 17 containing the peripheral myelin protein 22 (PMP22) gene [3]. As a result, myelin stability is primarily affected whilst axonal degeneration occurs secondarily. No curative treatment is currently available and an interventional

Correspondence: S. Attarian, Reference Center for Neuromuscular Diseases and ALS, La Timone University Hospital, Aix-Marseille University, 264 rue Saint Pierre, 13385 Marseille, France (tel.: +33 4 91 38 65 79; fax: +33 4 91 42 68 55; e-mail: sattarian@ap-hm.fr).

strategy aimed at stopping or slowing the disease progression has proved inefficient. Accordingly, the therapeutic potential of various compounds such as ascorbic acid [4–7] or a combination of ascorbic acid, naltrexone and baclofen [8,9] has been described. One of the major difficulties reported in these trials was to detect a potential early therapeutic response using the current clinical and electrophysiological tests [10]. A clinical validated score in CMT1A patients such as the CMT Neuropathy Score version 2 (CMTNSv2) [11] and the Overall Neuropathy Limitations Scale (ONLS) [12] has proved to be poorly sensitive to disease progression [13,14]. Nerve conduction measurements are limited to distal nerves that are often severely damaged and unexcitable at first evaluation [15]. In that context, sensitive biomarkers are warranted so that disease progression and the efficiency of potential therapeutic strategies can be assessed [16].

Quantitative magnetic resonance imaging (qMRI) techniques have been used in CMT over the past few years and structural abnormalities have been reported in nerves and muscles of the lower limbs, both proximally and distally [17]. Skeletal muscle MRI of the lower limbs showed a significantly increased fat fraction with a length-dependent peroneal-type pattern [18] and a high sensitivity to change over a 1-year period [19]. Regarding the nerve pathological involvement, various metrics such as nerve volume [20], proton density (PD) [21] and magnetization transfer ratio (MTR) [22] have been quantified, but the proximal-to-distal pattern of the sciatic and tibial nerves has not been specifically analyzed so that the most relevant area for MR neurography remains unknown.

The objective of the present study was to quantify the 3D nerve volume, MTR and PD using qMRI in CMT1A patients and to assess the potential proximal-to-distal gradient for the lower limb, i.e. thigh and leg. Correlations with conventional scores were investigated in order to identify the biomarkers of interest which could be used to monitor the natural progression of the disease and the efficiency of potential therapeutic strategies.

Methods

Clinical assessment

Thirty-two consecutive genetically confirmed CMT1A adult patients and 13 age and sex-matched controls were enrolled in this study from March 2016 to March 2018 in the Reference Center for Neuromuscular Disease and ALS (Marseille, France). Clinical evaluation included demographic data, neurological examination

and medical history. Muscle strength was evaluated through the Medical Research Council (MRC) scale [23]. Disease severity was assessed on the basis of the CMTNSv2 score, a composite score combining symptoms, signs and electrophysiological evaluation [11]. Another clinical score, without electrophysiological testing, referred to as the Charcot–Marie–Tooth examination score (CMTES) was also used together with the motor items of the leg (CMTES_L). Functional disability in daily life was recorded using the ONLS and its lower limb subpart (ONLS_L) [12].

Patients also underwent an electrophysiological examination, with compound motor action potential and Motor Unit Number Index measurements on the non-dominant muscles abductor pollicis brevis, abductor digiti minimi and tibialis anterior, as described in a previous study [19].

No patient had any history of other conditions. Standard biological tests were performed in order to rule out any disease linked to peripheral neuropathies such as diabetes or renal failure. The control group showed no medical history of neuromuscular disease. Informed consent was obtained from all participants and approval from the local ethics committee was obtained (IRB #2015-A00799-40).

Magnetic resonance neurography protocol

Magnetic resonance imaging was performed at 1.5 T (Siemens Avanto scanner). Patients lay supine whilst the leg and thigh of the non-dominant limb were imaged using a combination of multi-channel flexible coils (Siemens, Erlangen, Germany) on the top and spine coils (Siemens) integrated in the scanner bed. After a localizer, sets of images were recorded in the axial plane in order to quantify the sciatic and tibial nerve volumes [gradient recalled echo (GRE) sequence with selective water excitation], the corresponding PD (multi-echo turbo spin echo sequence) and the MTR (GRE with and without a saturation pulse). The nerve volume was quantified over pre-determined regions of interest (ROIs) covering a 20 cm distance and centered in the mid-thigh (presence of the short head of the biceps femoris muscle) and mid-leg (largest cross-sectional area) regions. From each MRI sequence recorded, a quantitative map was generated which was computed using various bias corrections. Details of the corresponding sequences are provided in Table 1.

Data processing

Nerve segmentation

The sciatic and tibial nerve contours were manually drawn in all 36 slices as the two ROIs on the 3D

Table 1 Parameters of the MRI sequences

	TR (ms)	TE (ms)	Voxel size (mm ²)	Slice thickness	Number of slices
3D GRE WE	16	6.97	0.5*0.5	5	36
2D TSE	2700	from 8.7 to 139.2	1.7*1.7	10	10
3D GRE with and without a saturation pulse ^a	36	3.5	1.7*1.7	5	36

GRE, gradient echo sequence; MRI, magnetic resonance imaging; TE, echo time; TR, repetition time; TSE, turbo spin echo; WE, water excitation. ^aThe saturation pulse was a 10-ms Gaussian pulse with a nominal 500° flip angle and a 1200 Hz offset frequency.

GRE dataset for both sciatic and tibial nerves [24] by an experienced Medical Doctor (MD) (EF, with greater than 5 years of experience) using FSLView (FSL, FMRIB Software Library, Oxford, UK) [25]. The most proximal (35) and the most distal (0) slices were excluded from the analysis given their poorer homogeneity. As illustrated in Fig. 1, the nerve borders were readily visible using the 3D water-selective GRE sequence. In the distal part of the thigh, the ROI included both branches of the sciatic nerve (peroneal and tibial), as described in a previous study [22]. Segmentation results were double checked by two experts (EF and AO). Both the 3D volume and the 3D mean cross-sectional area (CSA) were calculated for the two ROIs. The PD and MTR maps were linearly resized to the resolution of the 3D GRE dataset using FreeSurfer [26] so that each metric could be averaged over the whole set of segmented slices.

Proton density map

For each subject, the PD map was generated on a voxel basis using the signal intensity measured at each echo time on the turbo spin echo image. A multi-echo sequence with 17 echoes and an 8.7 ms echo spacing

was employed. Using a monoexponential equation, the corresponding intensities were fitted in order to produce a T2 map for each slice. The corresponding equation was used to extrapolate the signal intensity for a zero echo time on a voxel basis and generate a PD map for each slice.

Magnetization transfer ratio mapping

Magnetization transfer ratio quantification was performed as previously described [20]. Briefly, MTRs were computed on a voxel basis from the normalized difference between the intensity on the MT-weighted image ($I1$) acquired with a 3D fast low-angle shot readout (Table 1), preceded by a 10-ms Gaussian pulse with a nominal 500° flip angle and a 1200 Hz offset frequency, and the corresponding intensity on the image recorded without the saturation pulse ($I0$):

$$\text{MTR} = 100 * \left(1 - \frac{I0 - I1}{I0} \right)$$

A correction for the B1 inhomogeneities was performed as previously described [25] taking into account the B1 map.

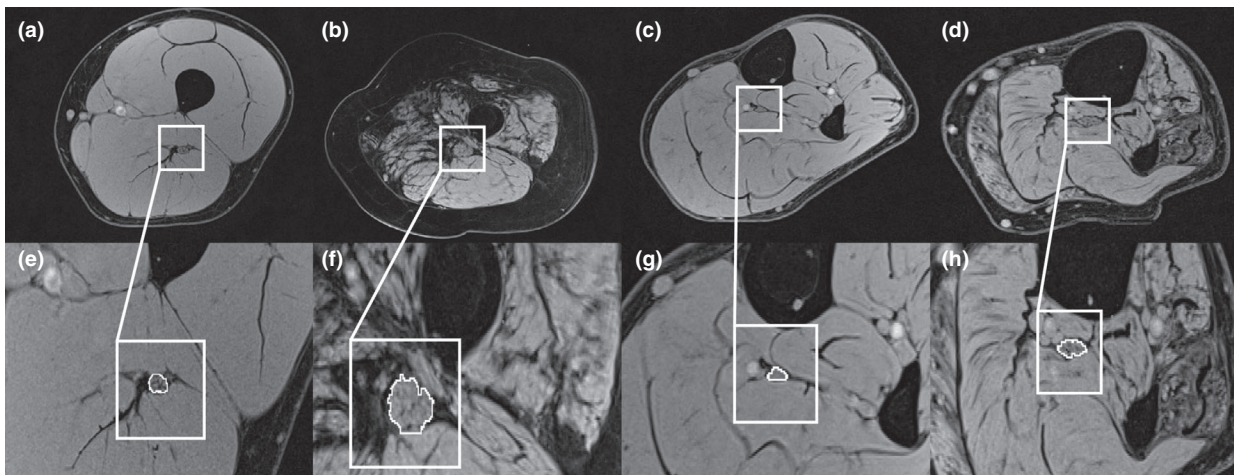


Figure 1 Typical MR images from a control (a, c, e, g) and a CMT patient (b, d, f, h). Images have been recorded at the thigh (a, b, e, f) and lower leg (c, d, g, h) levels. The lower panel illustrates an expanded region indicated as a white square.

Statistical analyses

Statistical analyses were performed using Addinsoft Xlstat (version 2018.7, Addinsoft, Bordeaux, France). Given the non-Gaussian distribution of the data, values were compared using nonparametric Wilcoxon–Mann–Whitney tests. The Spearman rank correlation (r) was used to analyze the correlations between metrics. Differences were considered as statistically significant for P values lower than 0.05. The results are presented as mean \pm SD.

Data availability statement

All de-identified data and related documentation from this study are available upon request to qualified researchers without limit of time, subject to a standard data sharing agreement.

Standard protocol approvals, registrations, and patient consents

This research protocol was approved by the French ethics committee (IRB #2015-A00799-40).

Results

Demographics and clinical data

Thirty-two patients (mean age 37.5 ± 13 years; 13 males) were included and compared to 13 controls (mean age 41.6 ± 13 years; seven males). There was no significant difference in age ($P = 0.53$) or sex ($P = 0.41$) between the two groups.

Charcot–Marie–Tooth type 1A patients displayed a typical phenotype of chronic length-dependent sensory–motor neuropathy with distal muscle weakness and deformities predominant in the lower limbs. Mean disease duration in patients was 25 years as first signs mostly appeared in childhood. Duplication of the PMP22 gene was confirmed in all patients.

Detailed clinical and demographic data with functional scores and MRC testing are presented in Table 2.

Magnetic resonance neurography measurements

The 3D nerve volume was significantly increased in patients compared to controls for the sciatic ($13\,002 \pm 4373$ mm³; 4989 ± 846 mm³; $P < 0.0001$) and tibial (4290 ± 1531 mm³; 1807 ± 258 mm³; $P < 0.0001$) nerves. The 3D mean CSA was also significantly higher in patients for sciatic (103.5 ± 25.7 mm²; 27.5 ± 5.0 mm²; $P < 0.0001$) and

Table 2 Demographic and clinical parameters of CMT1A patients

Variables	CMT1A patients
n (female/male)	32 (19/13)
Age (years)	37.5 ± 12.9
Disease duration (years)	25 ± 14
Functional scores	
CMTNSv2	13.6 ± 5.0
CMTES	9.7 ± 4.1
CMTES _L	3.4 ± 1.8
ONLS (UL–LL)	3.4 ± 1.3 (1.6/1.8)
MRC scores	
Quadriceps L/R	4.8/4.8
Psoas L/R	4.5/4.50
Plantar flexion L/R	3.8/3.8
Dorsal flexion L/R	3.8/3.8
DI L/R	3.7/3.5
CAPB	3.8/3.7

Data are expressed as mean \pm SD. CAPB, abductor pollicis brevis muscle; CMT1A, Charcot–Marie–Tooth type 1A; CMTES, Charcot–Marie–Tooth examination score; CMTES_L, Charcot–Marie–Tooth examination score (motor lower limb subpart); CMTNSvs2, Charcot–Marie–Tooth Neuropathy Score version 2; DI, first dorsal interosseous muscle; MRC score, Medical Research Council score; ONLS (UL–LL), Overall Neuropathy Limitations Scale (upper limb–lower limb).

tibial (38.9 ± 9.0 mm²; 10.6 ± 1.5 mm²; $P < 0.0001$) nerves.

Proton density was also significantly increased in patients for both nerve regions. Sciatic nerve PD (556.8 ± 88.9 ; 489.9 ± 64.5 ; $P = 0.0492$) and tibial nerve PD (550.7 ± 72.5 ; 492.3 ± 84.8 ; $P = 0.0417$) were both increased in the patient group.

A statistically significant difference was also demonstrated for the MTR with a reduction in the sciatic (33.7 ± 3.7 ; 39.5 ± 3 ; $P = 0.0025$) and the tibial nerves (41.5 ± 4.2 ; 44.2 ± 2.6 ; $P = 0.0449$) in CMT1A patients.

Given that the whole set of slices were segmented, the nerve volume proximal-to-distal gradient was analyzed. A physiological gradient was quantified in the thigh of controls with a larger nerve volume in the proximal area ($R^2 = 0.66$; $P < 0.0001$). This gradient was not found in patients with similar nerve volume and CSA values in the proximal and distal areas of the sciatic nerve ($R^2 = 0.03$; $P = 0.27$). At the leg level, no gradient was quantified in the control group ($R^2 = 0.01$; $P = 0.47$) whereas a slight and significant increase was quantified distally in the patient group ($R^2 = 0.55$; $P < 0.0001$).

In order to investigate whether the nerve alterations were more pronounced proximally or distally, the proximal-to-distal ratio, defined as the ratio between the proximal slices at the thigh level and the distal slices at the leg level, was computed for each metric.

Interestingly, there was no difference between CMT1A patients and controls for the proximal-to-distal ratio of volume [controls 3.34 ± 0.7 (4.20–2.32); CMT1A 3.38 ± 1.2 (5.35–1.46)] ($P = 0.86$), MTR [controls 0.83 ± 0.1 (0.99–0.65); CMT1A 0.70 ± 0.1 (0.88–0.30)] ($P = 0.07$) and PD [controls 0.92 ± 0.3 (1.68–0.71); CMT1A 0.74 ± 0.2 (1.13–0.52)] ($P = 0.13$).

The whole set of qMRI metrics are shown in Table 3 and Fig. 2.

Clinical correlations

As illustrated in Fig. 3, the 3D sciatic nerve volume was significantly correlated with the whole set of clinical scores: CMTNSv2 ($P = 0.018$; $\rho = 0.436$), CMTES ($P = 0.012$; $\rho = 0.459$), CMTES_L ($P = 0.045$; $\rho = 0.376$), ONLS ($P = 0.002$; $\rho = 0.552$) and ONLS_L ($P = 0.022$; $\rho = 0.423$). In contrast, no correlation was found between the tibial nerve volume and the clinical scores: CMTNSv2 ($P = 0.16$), CMTES ($P = 0.17$), CMTES_L ($P = 0.30$), ONLS ($P = 0.17$) and ONLS_L ($P = 0.76$).

Sciatic nerve PD was correlated with the ONLS ($P = 0.041$; $\rho = 0.383$) and the ONLS_L ($P = 0.005$; $\rho = 0.509$) whilst the sciatic nerve MTR was correlated with the quadriceps MRC score ($P = 0.0032$; $\rho = 0.053$). A significant relationship was also found between the tibial nerve MTR and the ONLS ($P = 0.029$; $\rho = -0.42$).

DISCUSSION

The present results further demonstrate that qMRI is able to provide sensitive quantitative biomarkers in CMT1A patients. It is noteworthy that using the GRE sequence combined with a water-selective excitation scheme, high-quality images were obtained at 1.5 T. Based on original measurements at the thigh and leg levels, significant differences between CMT1A patients and controls were reported regarding 3D nerve volume, MTR and PD for the whole sciatic and tibial nerve volume. On the basis of a 3D multi-slice analysis and the corresponding correlations with conventional clinical scores, our results strongly suggest that qMRI measurements at the thigh level might be the most appropriate in order to assess both natural disease progression and the potential efficiency of therapeutic strategies.

The sciatic and tibial nerve volume hypertrophy reported is in line with several previous studies [20,22]. Nerve hypertrophy is a well-known feature of CMT1A patients which has been linked to an increase of endoneurial collagen and the demyelination and remyelination processes giving the classic ‘onion bulb’ aspect in microscopy studies [24]. The nerve volume quantified was more than twice as large in patients as controls. Accordingly, the CSA of the sciatic nerve reported by Sinclair *et al.* [20] in a single slice from CMT1A patients was more than twice the size of

Table 3 Nerve metrics of CMT1A patients and healthy controls

	Thigh			Leg		
	CMT1A patients	Healthy controls	<i>P</i> value	CMT1A patients	Healthy controls	<i>P</i> value
Total volume (mm ³)	13 002 ± 4373	4989 ± 846	<0.0001	4290 ± 1531	1807 ± 258	<0.0001
Proton density	556.8 ± 88.9	489.9 ± 64.5	0.0492	550.7 ± 72.5	492.3 ± 84.8	0.0417
MTR	33.7 ± 3.7	39.5 ± 3	0.0025	41.5 ± 4.2	44.2 ± 2.6	0.0449

Data are expressed as mean ± SD. CMT1A, Charcot–Marie–Tooth type 1A; MTR, magnetization transfer ratio.

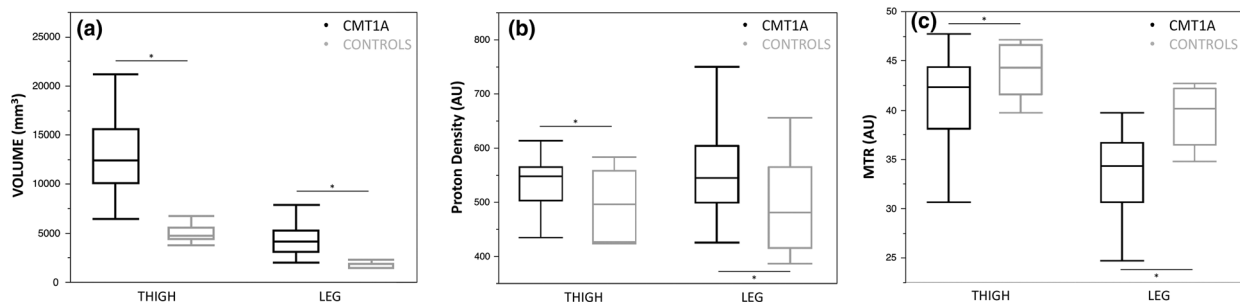


Figure 2 Nerve volume (a), proton density (b) and MTR (c) in controls (grey box plots) and patients (black box plots). Values have been quantified at the thigh and lower leg levels.

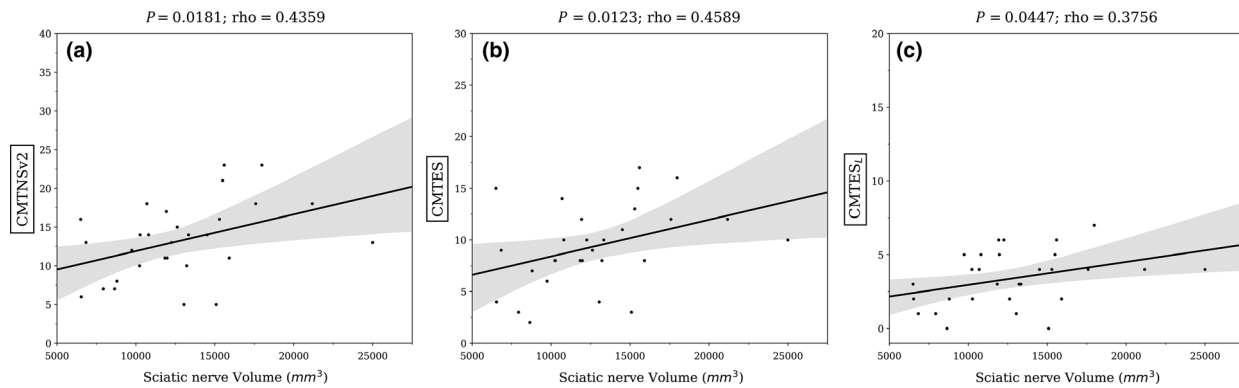


Figure 3 Relationships between sciatic nerve volume (mm^3) and clinical scores, i.e. CMTNSv2 (a), CMTES (b) and CMTES_L (c). *P* and rho values are indicated at the top. CMTNSv2, CMT Neurological Score version 2; CMTES, CMT examination score; CMTES_L, CMT examination score with the motor items of the leg.

controls. Vaeggemose *et al.* [21] reported a similar observation for a 4.8 cm nerve section. Considering our 3D analysis, it was determined that this hypertrophy occurred both proximally and distally.

In addition to the morphometric changes, PD was also significantly increased in the patient group. Such an increase has been previously reported once [21] in CMT1A patients at the thigh level and explained as a possible disease process more pronounced proximally than distally. Our results indicate that PD was increased at both thigh and leg levels. PD has been described as a sensitive microstructural biomarker of nerve tissue integrity in the peripheral nervous system which would reflect the macromolecular composition of nerves and muscles [27,28]. A PD elevation in peripheral nerves has already been reported in various neuropathies such as diabetes [29] and familial amyloid polyneuropathy [30]. It might be linked to protein deposits or inflammatory reactions in the extracellular matrix [31]. In amyloidosis, the accretion of unfolded transthyretin deposits in the endoneurium has been suggested as a potential accounting factor of PD augmentation. In the context of CMT1A, PD elevation might be secondary to the above-normal thickness sheaths of myelin. The exact interpretation of structural changes leading to PD alterations would have to be complemented by anatomic-pathological evaluations.

The MTR, another metric related to the macromolecular content of the nerve, was also reduced in patients for both sciatic and tibial nerves. According to previous imaging studies, the nerve MTR could be affected by myelin lipid composition and would therefore be sensitive to changes in myelin density [32]. MTR changes have been investigated in the peripheral nervous system [33] and only a single study has described pathological modifications in the sciatic

nerve of CMT1A patients [22]. The corresponding 33% MTR reduction in the patient group is consistent with our results. The significant MTR reduction reported in the tibial nerve of patients has never been recorded before and probably reflects myelin density alterations in both thigh and leg levels that are known to disrupt axon–Schwann cell interactions causing nerve dysfunction. Both results indicate the presence of microstructural abnormalities along the whole nerve.

In the present study, it was possible to assess the proximal-to-distal gradient of the quantitative nerve parameters in both thigh and leg compartments. In CMT1A, the length-dependent pattern of the muscular impairment was well established since the first clinical descriptions, with distal sensory–motor deficit and atrophy. MRI studies have also illustrated this specific feature with larger degeneration in intrinsic foot muscles [33]. More recently, using a 3D analysis, a length-dependent profile of the muscle fat infiltration has been reported with a predominant involvement of the leg compared to the thigh compartment [18]. This length-dependent profile initially reported in the muscle tissue was not observed in the sciatic and tibial nerves whilst a global and major hypertrophy was quantified in the whole limb of the patients. Interestingly, the sciatic nerve volume was strongly correlated with the whole set of clinical scores whereas tibial nerve volume was not. This might result from the secondary axonal loss which is known to occur in nerve extremities of CMT1A patients [34]. This additional process would lead to a distal nerve volume diminution thereby affecting correlations at the leg level. In CMT1A patients, the leg area is also problematic for nerve conduction velocity measurements whilst non-responsive distal sensory nerves account for the floor effect in longitudinal studies [35]. Significant

differences in MTR and PD were also identified at the thigh level in our patient cohort. In addition, correlations between sciatic nerve volume and CMTNSv2 scores were recorded in the thigh compartment. Altogether, this would support the potential use of MRI metrics in the proximal compartment as biomarkers for further studies. This would overcome the problem of distal nerve degeneration in CMT1A. From a methodological point of view, the sciatic diameter measurement is easier given its larger dimension and one might expect a more accurate segmentation and a lower sensitivity to potential subject motions during the MRI scanning. Biological and nerve-related MRI parameters have been previously correlated in diabetic patients [36] and this type of correlation was not found in our patients who did not suffer from diabetes.

Whilst the analyzed tridimensional region of interest using MRI was large and the number of CMT1A patients enrolled in this study was quite important, a few limitations must be acknowledged. As diffusion tensor imaging was not used, it was not possible to assess the sciatic nerve's fractional anisotropy [21]. T2 measurements using multi-echo spin echo methods can suffer from stimulated echo artefacts and affect the corresponding quantification [37]. As a mixture of fat and water was not expected in the nerve region, a bi-exponential fitting taking into account the fat fraction was not used but only a single exponential fitting method. The corresponding correlation coefficients were always larger than 0.95 thereby illustrating a minor stimulated echo effect which should at least be similar for all the subjects.

It would be of interest to investigate the effects of genetic mutations [38] and age [39]. The reproducibility of our segmentation approach has been demonstrated previously [40] and a longitudinal study would be required to analyze the relevance of the MRI metrics selected for the assessment of the natural progression of the disease and the potential efficiency of therapeutic strategies.

In conclusion, qMRI combined with a 3D segmentation approach can be used to characterize *in vivo* nerve tissue using several sensitive morphometric and structural parameters that correlate with disability in CMT1A patients. The sensitivity of the selected metrics would have to be assessed through repeated measurements over time during longitudinal studies to evaluate structural nerve changes under treatment.

Acknowledgement

Centre National de La Recherche Scientifique UMR 7339.

Disclosure of conflicts of interest

None of the authors has any disclosure to report.

References

1. Szigeti K, Lupski JR. Charcot–Marie–Tooth disease. *Eur J Hum Genet* 2009; **17**: 703–710.
2. Barreto LC, Oliveira FS, Nunes PS, *et al.* Epidemiologic study of Charcot–Marie–Tooth disease: a systematic review. *Neuroepidemiology* 2016; **46**: 157–165.
3. Lupski JR, de Oca-Luna RM, Slaugenhaupt S, *et al.* DNA duplication associated with Charcot–Marie–Tooth disease type 1A. *Cell* 1991; **66**: 219–232.
4. Burns J, Ouvrier RA, Yiu EM, *et al.* Ascorbic acid for Charcot–Marie–Tooth disease type 1A in children: a randomised, double-blind, placebo-controlled, safety and efficacy trial. *Lancet Neurol* 2009; **8**: 537–544.
5. Lewis RA, McDermott MP, Herrmann DN, *et al.* High-dosage ascorbic acid treatment in Charcot–Marie–Tooth disease type 1A: results of a randomized, double-masked, controlled trial. *JAMA Neurol* 2013; **70**: 981–987.
6. Micallef J, Attarian S, Dubourg O, *et al.* Effect of ascorbic acid in patients with Charcot–Marie–Tooth disease type 1A: a multicentre, randomised, double-blind, placebo-controlled trial. *Lancet Neurol* 2009; **8**: 1103–1110.
7. Verhamme C, de Haan RJ, Vermeulen M, Baas F, de Visser M, van Schaik IN. Oral high dose ascorbic acid treatment for one year in young CMT1A patients: a randomised, double-blind, placebo-controlled phase II trial. *BMC Med* 2009; **7**: 70.
8. Attarian S, Vallat JM, Magy L, *et al.* An exploratory randomised double-blind and placebo-controlled phase 2 study of a combination of baclofen, naltrexone and sorbitol (PXT3003) in patients with Charcot–Marie–Tooth disease type 1A. *Orphanet J Rare Dis* 2014; **9**: 199.
9. Chumakov I, Milet A, Cholet N, *et al.* Polytherapy with a combination of three repurposed drugs (PXT3003) down-regulates Pmp22 over-expression and improves myelination, axonal and functional parameters in models of CMT1A neuropathy. *Orphanet J Rare Dis* 2014; **9**: 201.
10. Gess B, Baets J, De Jonghe P, Reilly MM, Pareyson D, Young P. Ascorbic acid for the treatment of Charcot–Marie–Tooth disease. *Cochrane Database Syst Rev* 2015; **12**: CD011952.
11. Murphy SM, Herrmann DN, McDermott MP, *et al.* Reliability of the CMT neuropathy score (second version) in Charcot–Marie–Tooth disease. *J Peripher Nerv Syst* 2011; **16**: 191–198.
12. Graham RC, Hughes RA. A modified peripheral neuropathy scale: the Overall Neuropathy Limitations Scale. *J Neurol Neurosurg Psychiatry* 2006; **77**: 973–976.
13. Mandel J, Bertrand V, Leheret P, *et al.* A meta-analysis of randomized double-blind clinical trials in CMT1A to assess the change from baseline in CMTNS and ONLS scales after one year of treatment. *Orphanet J Rare Dis* 2015; **10**: 74.
14. Pareyson D, Reilly MM, Schenone A, *et al.* Ascorbic acid in Charcot–Marie–Tooth disease type 1A (CMT-TRIAL and CMT-TRAUK): a double-blind randomised trial. *Lancet Neurol* 2011; **10**: 320–328.

15. Manganelli F, Pisciotta C, Reilly MM, *et al.* Nerve conduction velocity in CMT1A: what else can we tell? *Eur J Neurol* 2016; **23**: 1566–1571.
16. Morrow JM, Sinclair CD, Fischmann A, *et al.* Reproducibility, and age, body-weight and gender dependency of candidate skeletal muscle MRI outcome measures in healthy volunteers. *Eur Radiol* 2014; **24**: 1610–1620.
17. Morrow JM, Sinclair CD, Fischmann A, *et al.* MRI biomarker assessment of neuromuscular disease progression: a prospective observational cohort study. *Lancet Neurol* 2016; **15**: 65–77.
18. Bas J, Ogier AC, Le Troter A, *et al.* Fat fraction distribution in lower limb muscles of CMT1A patients: a quantitative MRI study. *Neurology* 2020; **94**: e1480–e1487.
19. Morrow JM, Evans MRB, Grider T, *et al.* Validation of MRC Centre MRI calf muscle fat fraction protocol as an outcome measure in CMT1A. *Neurology* 2018; **91**: e1125–e1129.
20. Sinclair CD, Morrow JM, Miranda MA, *et al.* Skeletal muscle MRI magnetisation transfer ratio reflects clinical severity in peripheral neuropathies. *J Neurol Neurosurg Psychiatry* 2012; **83**: 29–32.
21. Vaeggemose M, Vaeth S, Pham M, *et al.* Magnetic resonance neurography and diffusion tensor imaging of the peripheral nerves in patients with Charcot–Marie–Tooth type 1A. *Muscle Nerve* 2017; **56**: E78–E84.
22. Dortch RD, Dethrage LM, Gore JC, Smith SA, Li J. Proximal nerve magnetization transfer MRI relates to disability in Charcot–Marie–Tooth diseases. *Neurology* 2014; **83**: 1545–1553.
23. Compston A. Aids to the investigation of peripheral nerve injuries. Medical Research Council: Nerve Injuries Research Committee. His Majesty's Stationery Office: 1942; pp. 48 (iii) and 74 figures and 7 diagrams; with aids to the examination of the peripheral nervous system. By Michael O'Brien for the Guarantors of Brain. Saunders Elsevier: 2010; pp. [8] 64 and 94 Figures. *Brain* 2010; **133**: 2838–2844.
24. Duchesne M, Mathis S, Richard L, *et al.* Nerve biopsy is still useful in some inherited neuropathies. *J Neuropathol Exp Neurol* 2018; **77**: 88–99.
25. Jenkinson M, Beckmann CF, Behrens TE, Woolrich MW, Smith SM. Fsl. *NeuroImage* 2012; **62**: 782–790.
26. Fischl B. FreeSurfer. *NeuroImage* 2012; **62**: 774–781.
27. Walimuni IS, Hasan KM. Atlas-based investigation of human brain tissue microstructural spatial heterogeneity and interplay between transverse relaxation time and radial diffusivity. *NeuroImage* 2011; **57**: 1402–1410.
28. Miot E, Hoffschir D, Alapetite C, *et al.* Experimental MR study of cerebral radiation injury: quantitative T2 changes over time and histopathologic correlation. *AJNR Am J Neuroradiol* 1995; **16**: 79–85.
29. Jende JME, Groener JB, Oikonomou D, *et al.* Diabetic neuropathy differs between type 1 and type 2 diabetes: insights from magnetic resonance neurography. *Ann Neurol* 2018; **83**: 588–598.
30. Kollmer J, Hund E, Hornung B, *et al.* *In vivo* detection of nerve injury in familial amyloid polyneuropathy by magnetic resonance neurography. *Brain* 2015; **138**(Pt 3): 549–562.
31. Tofts PS, du Boulay EP. Towards quantitative measurements of relaxation times and other parameters in the brain. *Neuroradiology* 1990; **32**: 407–415.
32. Odrobina EE, Lam TY, Pun T, Midha R, Stanisiz GJ. MR properties of excised neural tissue following experimentally induced demyelination. *NMR Biomed* 2005; **18**: 277–284.
33. Gambarota G, Veltien A, Klomp D, Van Alfen N, Mulkern RV, Heerschap A. Magnetic resonance imaging and T2 relaxometry of human median nerve at 7 Tesla. *Muscle Nerve* 2007; **36**: 368–373.
34. Krajewski KM, Lewis RA, Fuerst DR, *et al.* Neurological dysfunction and axonal degeneration in Charcot–Marie–Tooth disease type 1A. *Brain* 2000; **123**(Pt 7): 1516–1527.
35. Piscosquito G, Reilly MM, Schenone A, *et al.* Responsiveness of clinical outcome measures in Charcot–Marie–Tooth disease. *Eur J Neurol* 2015; **22**: 1556–1563.
36. Tozza S, Bruzzese D, Pisciotta C, *et al.* Motor performance deterioration accelerates after 50 years of age in Charcot–Marie–Tooth type 1A patients. *Eur J Neurol* 2018; **25**(2): 301–306.
37. Ben-Eliezer N, Sodickson DK, Block KT. Rapid and accurate T2 mapping from multi-spin-echo data using Bloch-simulation-based reconstruction. *Magn Reson Med* 2015; **73**: 809–817.
38. Berciano J, Garcia A, Gallardo E, *et al.* Intermediate Charcot–Marie–Tooth disease: an electrophysiological reappraisal and systematic review. *J Neurol* 2017; **264**: 1655–1677.
39. Jende JME, Groener JB, Kender Z, *et al.* Troponin T parallels structural nerve damage in type 2 diabetes: a cross-sectional study using magnetic resonance neurography. *Diabetes* 2020; **69**: 713–723.
40. Ogier A, Sdika M, Foure A, Le Troter A, Bendahan D. Individual muscle segmentation in MR images: a 3D propagation through 2D non-linear registration approaches. Conference proceedings : Annual International Conference of the IEEE Engineering in Medicine and Biology Society IEEE Engineering in Medicine and Biology Society Annual Conference. 2017; **2017**: 317–320.